Microstructure and Sliding Wear Resistance of Laser Cladded WC/Ni Composite Coatings with Different Contents of WC Particle

J.S. Xu, X.C. Zhang, F.Z. Xuan, Z.D. Wang, and S.T. Tu

The aim of this article was to address the effect of WC content on the microstructure, microhardness, and sliding wear resistance of laser cladded WC/Ni composite coatings. The content of WC particle in the feed powder varied in the range of 0-80 wt.%. Experimental results showed that the laser cladded coatings exhibited homogeneous microstructure without pores or cracks. By comparing with the 45# steel substrate, the microhardness of WC/Ni composite coatings was relatively high. The microhardness of coating increased with increasing the content of WC particles. The wear resistance of WC/Ni composite coatings was strongly dependent on the content of WC particle and their microstructure. When the WC content was lower than 40 wt.% in the feed powder, the wear rate of the coatings decreased with increasing WC content. The two-body abrasive wear was identified as the main wear mechanisms. For the coatings with WC content higher than 40 wt.% in the feed powder, their wear rate increased with increasing WC content. The three-body abrasive wear and fatigue wear were the main failures. The coating with 40 wt.% WC in the feed powder exhibited the best wear resistance.

Keywords	coatings, metal matrix composites, wear

1. Introduction

Many components such as cutting tools and mining machinery parts are subjected to premature failure due to the surface damage in sliding contact. Generally, these damages are limited to the near surface layer of bodies, which leads to an increasing demand in the surface engineering industry to improve the wear and corrosion resistance to meet demanding operating environments. Surface coating is nowadays being more and more considered as an effective and economical means to extend the service life of the components and to improve durability and product reliability.

Thermal spraying has been widely used to deposit coatings to protect the substrates from sliding wear and to improve the wear resistance of substrates. Nevertheless, the defect-free coatings were not likely to be obtained even when the latest thermal spraying techniques were applied (Ref 1). Generally, pores, microcracks, splat boundaries, and some unmelted particles would be generated in thermal sprayed coatings which can be characterized by lamellar structure due to the nature of the coating process (Ref 2, 3). Moreover, the bonding strength between the coating and the substrate is relatively low because of the mechanical bond at the interface (Ref 4, 5). The

existences of these micro-defects may limit the use of the thermal sprayed coatings to low-stress applications. Therefore, in order to improve the microstructural integrity and wear resistance of surface coatings, some high energy beam techniques, such as laser cladding, have been developed to deposit surface coatings. The pore- and crack-free coatings can be obtained due to heat concentrating and high cooling rate in laser cladding process (Ref 6). The high wear resistance of the cladded coatings can also be reached, since they are generally metallurgically bonded onto the substrates.

Among the materials used for laser cladding, Ni-based self-fluxing alloys have been extensively used due to their high intensity, toughness, and corrosion resistances (Ref 7-9). However, the low hardness and poor wear resistance prevent their applications as engineering tribological components under high-loading conditions. Tungsten carbide as a hard phase is often added into the Ni matrix to improve the wear resistance of Ni-based alloy coatings. So far, numerous researches have been concentrated on the wear resistance and related failure mechanisms of laser cladded WC/Ni coatings (Ref 10-15). For instance, Huang et al. (Ref 13) investigated the effect of laser cladded WC/Ni coatings on the wear resistance of H13 tool steel and found that the wear resistance of the coatings was a factor of 5-10 higher than that of as-received H13 tool steel. Chen et al. (Ref 14) found that the element diffusion and a new phase precipitation occurred during the sliding wear of laser cladded WC/Ni60B coatings. Van Acker et al. (Ref 15) investigated the influence of the size and distribution of tungsten carbide particles on the wear resistance of laser cladded WC/Ni coatings. They found that the size and distribution of tungsten carbide particles might have important influences on the failure mode of coating. However, the researches regarding the effect of content of WC particle on the wear resistance of WC/Ni composite coatings were very few. Hence, the aim of this article

J.S. Xu, X.C. Zhang, F.Z. Xuan, Z.D. Wang, and **S.T. Tu**, Key Laboratory of Pressurized System and Safety, Ministry of Education, East China University of Science and Technology, Shanghai 200237, People's Republic of China. Contact e-mails: xczhang@ecust.edu.cn and fzxuan@ecust.edu.cn.

was to address the effect of WC content on the microstructure, microhardness, and sliding wear resistance of laser cladded WC/Ni composite coatings. The coatings were prepared through changing the weight percentage of WC particle in the WC/Ni feed powder during laser cladding.

2. Experimental Procedures

2.1 Materials and Coating Preparation

In this study, a mixture of commercially available Ni-Cr-B-Si-W-C powder (Ni60) of nominal composition of Cr-15.50, Fe-15.00, Si-4.00, B-3.50, W-3.00, C-0.80, Ni-balance (wt.%), and WC powder consisting of cast carbide grains was used as feedstock material in laser cladding. These powders were prepared by Beijing General Research Institute of Mining and Metallurgy, China. The size of the Ni60 powder particles was in the range of 44 to 100 μm and that of WC powder particles was in the range of 44 to 74 μm. The morphologies of these powders are illustrated in Fig. 1, which showed that the Ni60 and WC powders were characterized by near-perfect spherical particles.

The substrate material used was a commercial middle carbon steel, which was cut to yield $30 \times 30 \times 15$ mm specimens. Prior to cladding, one face of the steel substrate was cleaned in acetone solution, sandblasted by using corundum powder and then preheated to 100-200 °C to avoid the generation of cracks in the laser cladded coating. For sandblasting and laser cladding, the substrates were fixed by the corresponding fixtures.

The laser cladded coatings with different WC contents of 0, 20, 40, 60, and 80 wt.% in the feed powder were prepared by using a 4 kW continuous wave CO_2 laser system fabricated by Shanghai Unity Prima Limited Company, China. The laser output power used in the experiments was in the range of 2.0-2.8 kW with a laser beam size of 6×2 mm. During laser cladding, the powder was supplied coaxially in situ around the laser beam and argon gas was blown to shroud the molten pool. The optimized processing parameters used in laser cladding are listed in Table 1.

2.2 Characterization of Coating

The microstructure of coatings was observed through a JSM-6360LV scanning electron microscopy (SEM). X-ray diffraction (XRD) with Cu Kα radiation and step 0.02° was used to identify the crystal structure of the coatings. Microhardness of the coatings was measured through an HXD-1000TM instrument with a 1000 gf load. The worn surface and cross-sectional morphologies of the failed coatings were observed by using the SEM as well.

2.3 Sliding Wear Tests

The sliding wear tests were performed on a ring-on-block tester of MM200 controlled by a computer, as shown in Fig. 2. The lower sample, Si_3N_4 ceramic rings with 40 mm in outer diameter, 16 mm in inner diameter, 10.8 mm in width, rotated at 200 rpm, resulting in a relative sliding speed of 0.425 m/s during sliding. As for the upper sample, block-like specimen ($30 \times 30 \times 10$ mm in size) coated with WC/Ni composite coatings which was fixed on the sample holder was pressed under applied loads of 400 N. Prior to sliding test, the specimen was ground and polished to attain a roughness (Ra) of around 0.35 μm at the coating surface, and then washed in ethanol. The total sliding distance for the test was 2500 m. At 500 m intervals, the weight losses of the specimen were measured and recorded. The wear mass loss of the samples was determined by an electronic analytical balance with an accuracy of 0.1 mg. To ensure the accuracy of measurement, the specimen was ultrasonically cleaned for 20 min before each weight measurement. The wear rates of the coatings with different contents of WC were calculated from the wear mass of the coatings. All tests were carried out at room temperature and atmospheric environment with lubrication (Machine Oil SEA 46). The lubricant had a kinematic viscosity of 46.91 cSt at 40 °C, a

Table 1 Optimized processing parameters used in laser cladding for the coatings with different WC contents in the feed powder

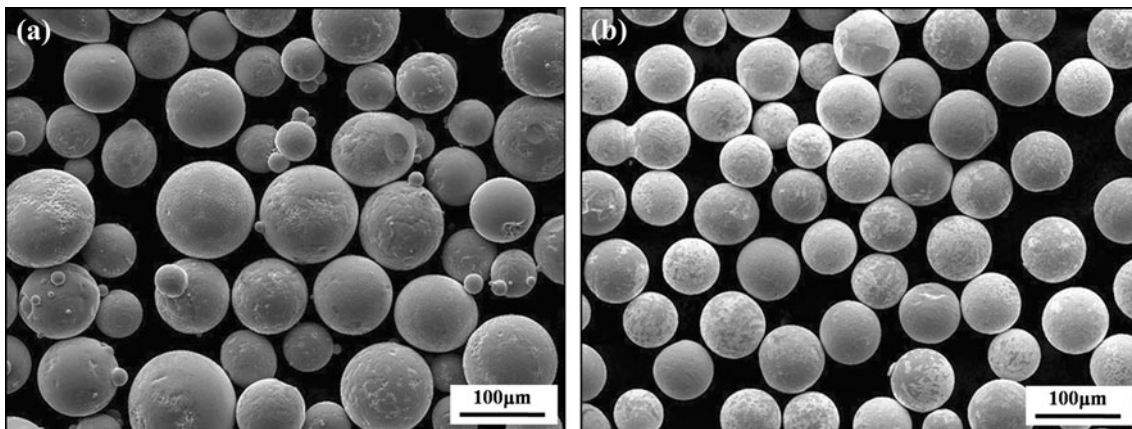| Content of carbides, wt.%	Laser power, W	Laser scanning speed, mm/s	Powder mass flow, g/min
0	2800	3	5.0
20	2600	4	6.5
40	2400	4	8.0
60	2200	4	9.5
80	2000	4	11.0

Fig. 1 The morphologies of the feed powders: (a) Ni60 and (b) WC
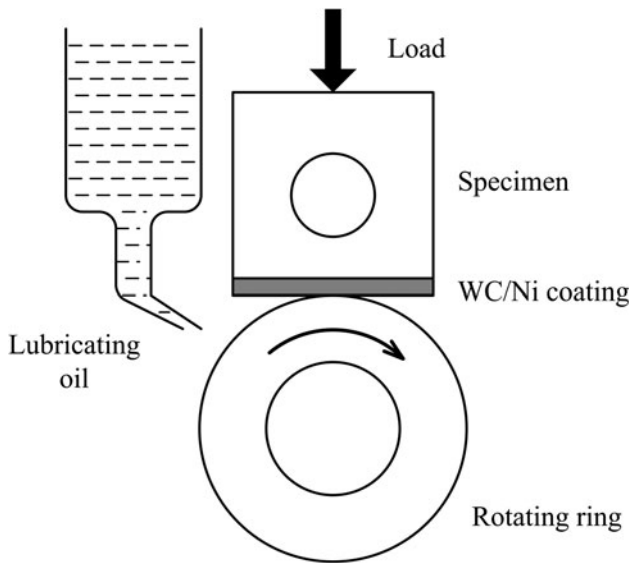
Fig. 2 Schematic diagram of MM200 sliding wear tester

viscosity index of 104, a flashing point of 207 °C, and a density of 0.874 g/cm^3 at 20 °C.

3. Results

3.1 Microstructure and Composition of Coatings

The cross-sectional images of the microstructure of the coatings with different contents of WC are revealed in Fig. 3. The thicknesses of the coatings are in the range of 300 to 400 μm. The bright phases of the coating consist mainly of WC. A lot of existing literatures have reported that reinforcement particles tended to sink and cluster towards the bottom of the coating owing to the lower melting points and slower solidification rates of the matrix (Ref 16-18). However, in this work, the distribution of WC particle is almost homogeneous throughout the coatings and the pores and cracks cannot be found in the coatings. These results indicate that the preheating treatment of substrate before cladding may be an effective approach to prevent the coatings from cracking and clustering.

A thin layer of planar crystallizing exists at the interface between the coating and the substrate, as shown in Fig. 4, indicating the metallurgical bonding at the interface. After laser cladding, the WC reinforcement particles keep initially spherical morphology in the coatings with low WC content, as seen in Fig. 4(a). A little dissolution of WC can be found at the edge of particles, which could improve the bonding strength between WC particle and Ni matrix. When the WC content in coating is relatively high (i.e., 80%), the WC particles are surrounded by numerous butterfly-like particles and dendritic phases, as seen Fig. 4(b). In such a case, the weight percentage of tungsten element in the butterfly-like particles is around 58%, which is measured by electronic differential system (EDS). This phenomenon may be attributed to the reaction between the molten Ni binder and the WC particles, resulting in the formation of intermetallic phases with a distinct butterfly-like or dendritic morphology.

The XRD patterns of the laser cladded WC/Ni composite coatings with different WC particle contents are shown in

Fig. 5. It can be seen that the crystalline phases of WC/Ni composite coating consist mainly of γ-Ni, WC, W$_2$C, Ni$_2$W$_4$C, Cr$_{23}$C$_6$, and Fe$_2$B. The XRD spectrum of Ni60 coating shows peaks completely indexed to γ-Ni. The existence of Ni$_2$W$_4$C suggests the formation of intermetallic phase in the matrix of the cladded coating. The intensity of the tungsten carbide phases increases with increasing the content of WC particle in the feed powder.

3.2 Microhardness Measurements

The microhardness profiles in the coatings along the depth are shown in Fig. 6. It can be seen that the microhardness of the coatings is obviously higher than that of the substrate. The microhardness of the Ni60 coating is relatively uniform along the depth direction, i.e., around 350 HV, which is lower than the microhardness of the WC/Ni coatings. Generally, the magnitude of microhardness of WC/Ni coating increases with increasing the WC content in coating. For the WC/Ni coatings, the cross-sectional microhardness of varies drastically with the depth of the coating, which may be attributed to the inhomogeneous distribution of the hard WC phase. Generally, the microhardness measurements are strongly dependent on indentation position for unhomogeneous microstructure (Ref 18). The similar result was also obtained by Tobar et al. (Ref 19).

3.3 Wear Resistance Analysis

The wear mass loss data of the laser cladding coating and substrate material as functions of the sliding distance are plotted in Fig. 7. For all the samples, the wear mass loss of wear surface almost linearly increases with sliding distance. By comparing with the 45# steel substrate, the wear resistance of the cladded coatings is relatively high. At a given wear distance, with increasing the content of WC particle in the WC/Ni coating, the wear loss of coating initially decreases and then increases. The coating with WC particle content of 40 wt.% in the feed powder exhibits the best wear resistance.

3.4 Worn Surface Morphologies

In order to understand the wear mechanism of the specimens, the worn surfaces of the coatings were examined by SEM, as seen in Fig. 8. Figure 8(a) shows the worn surface morphology of the 45# steel substrate after sliding test. The worn surface is characterized by deep and fairly long continuous grooves. This can probably be explained by the fact that silicon nitride has a relatively higher hardness than the 45# steel. At the beginning of the wear process, the hard protrusions on the rotating ring surface penetrate into the softer substrate surface and remove the materials at surface by such mechanisms as micro-cutting and micro-plowing. By comparing with the substrate material, the worn surface of the laser cladded Ni60 alloy coating is relatively smooth and shallow, as seen in Fig. 8(b). It can be explained by the fact that the hardness of Ni alloy coating is higher than that of 45# steel. Figure 8(c) shows the SEM morphology of the worn WC/Ni composite coating containing 20 wt.% WC after the sliding test. Micro-plowing and debris can be seen clearly on the wear track, indicating that the wear mechanism has changed from the two-body abrasive wear to the three-body abrasive wear by comparing with that of Ni60 alloy coating. In addition, the WC particles protrude from the worn surface, as a result of the removal of the matrix during sliding process. Worn surface observation of coating with WC content of 40 wt.% is shown in
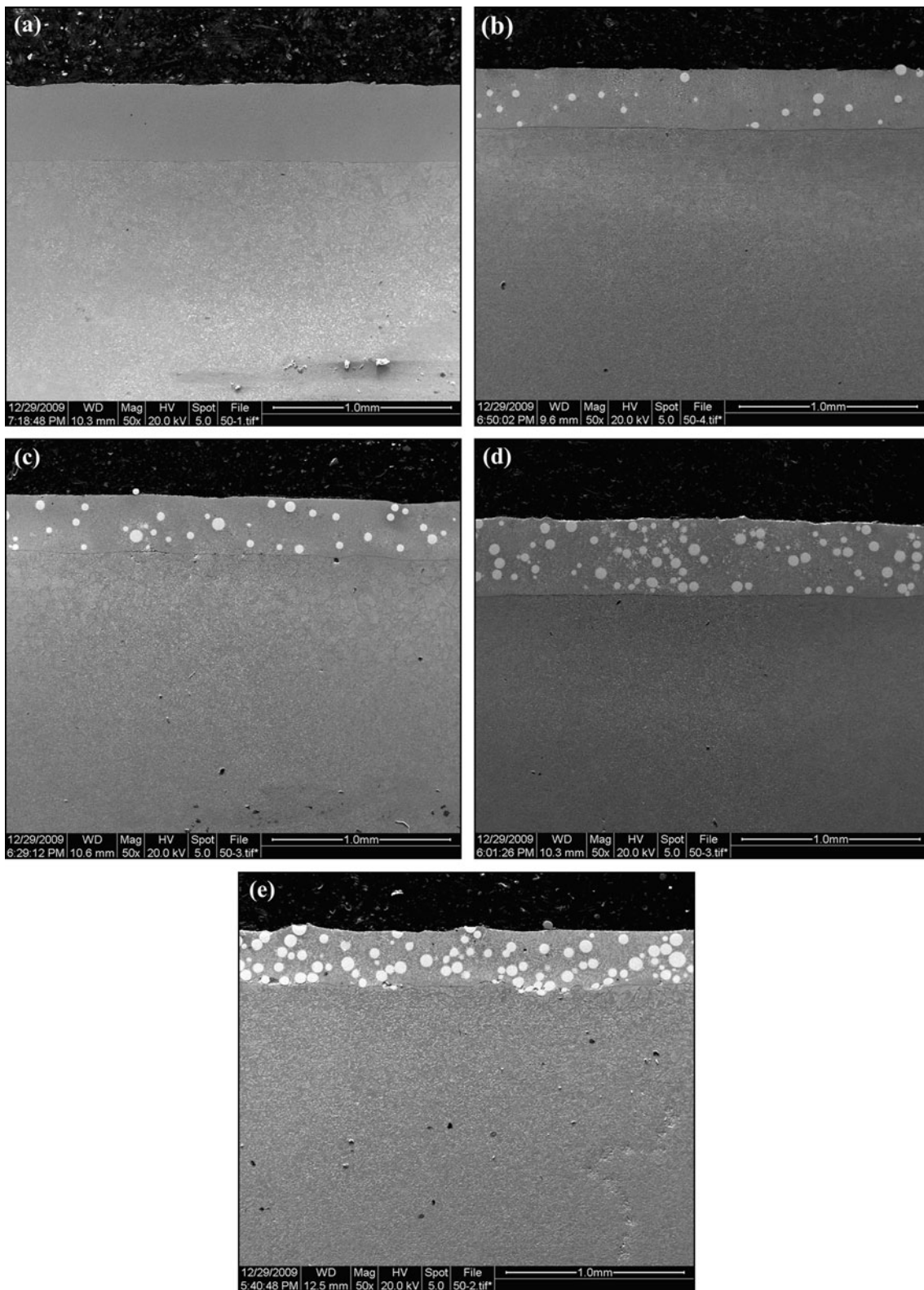
Fig. 3 Cross sections microstructure of the coatings with, (a) 0 wt.%, (b) 20 wt.%, (c) 40 wt.%, (d) 60 wt.%, and (e) 80 wt.% WC particles in the feed powder

Fig. 8(d). The track is characterized by parallel distributed ridges and grooves, and the amount of the hard debris on the worn surface is much higher than that observed on the worn surface of Ni60 alloy coating. This hard debris dropped from the

WC particle and the surface of the rotating ring during the sliding wear. A part of debris may lead to the damage of both surfaces, resulting in a third-body abrasive. Another part of debris may be pressed into the soft matrix under the high contact
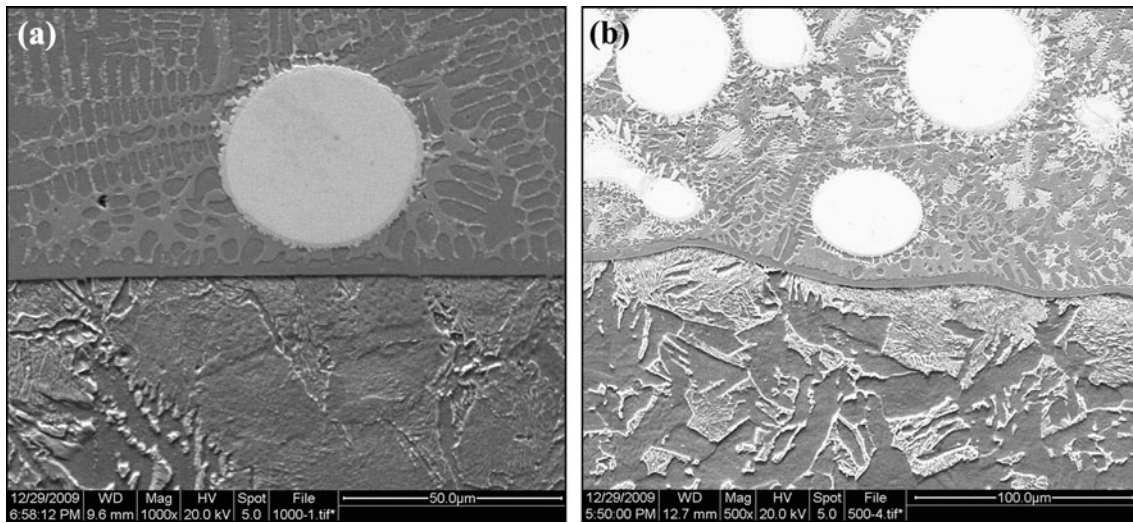
Fig. 4 Cross-sectional microstructure of near the interface between the cladded coating and the substrate at high magnification, (a) coating with 20 wt.% WC particles, and (b) coating with 80 wt.% WC particles
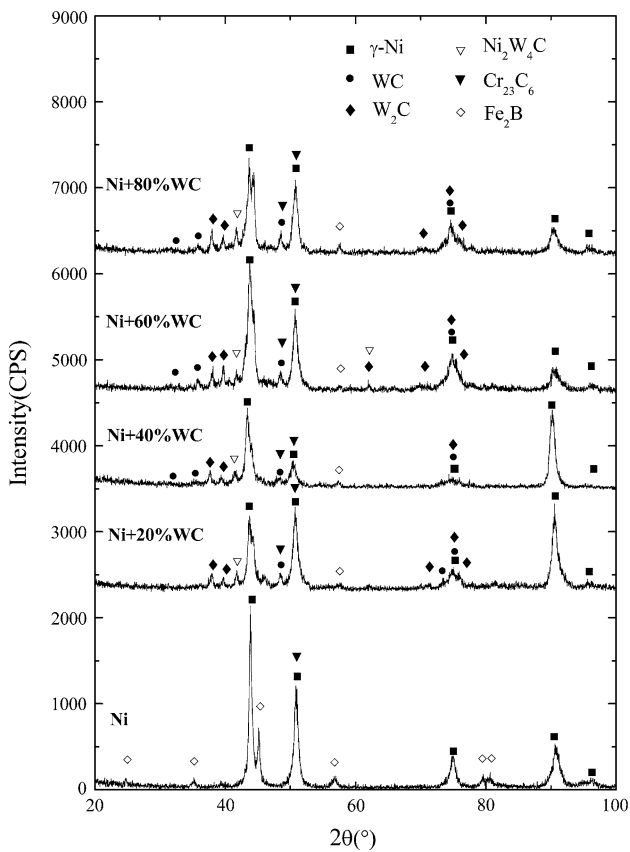

Fig. 5 XRD spectrums of the coatings with different contents of WC

Fig. 6 Profiles of through-thickness micro-hardness for the tested coatings with different WC contents

Fig. 7 Wear mass loss of the laser cladded coatings and the substrate as a function of the sliding distance

stress, as indicated by the arrow in Fig. 8(d). However, the WC particles protruding from the surface show few cracks and a good interfacial bond with Ni matrix.

The worn surface of the coating with 80 wt.% WC reinforcement particles is shown in Fig. 9. At a lower magnification in Fig. 9(a), a number of cavities on the scale of the original WC particle can be found at the worn surface,
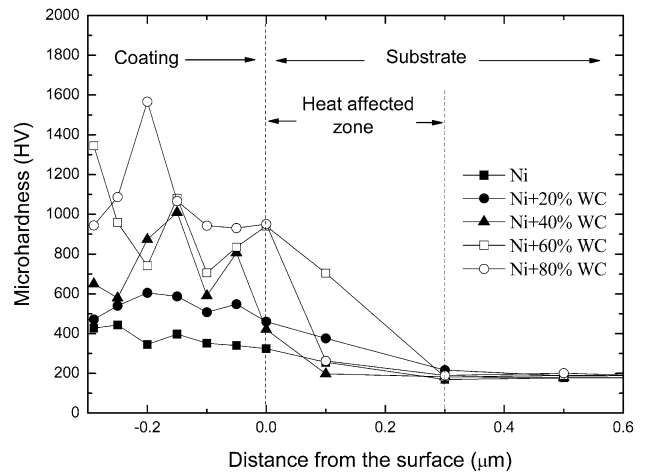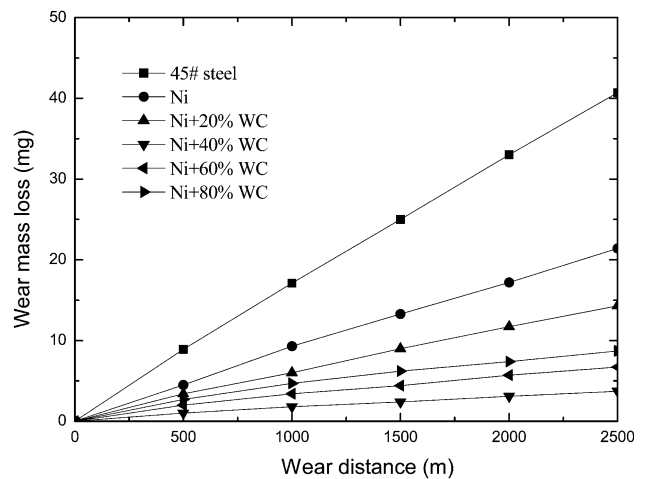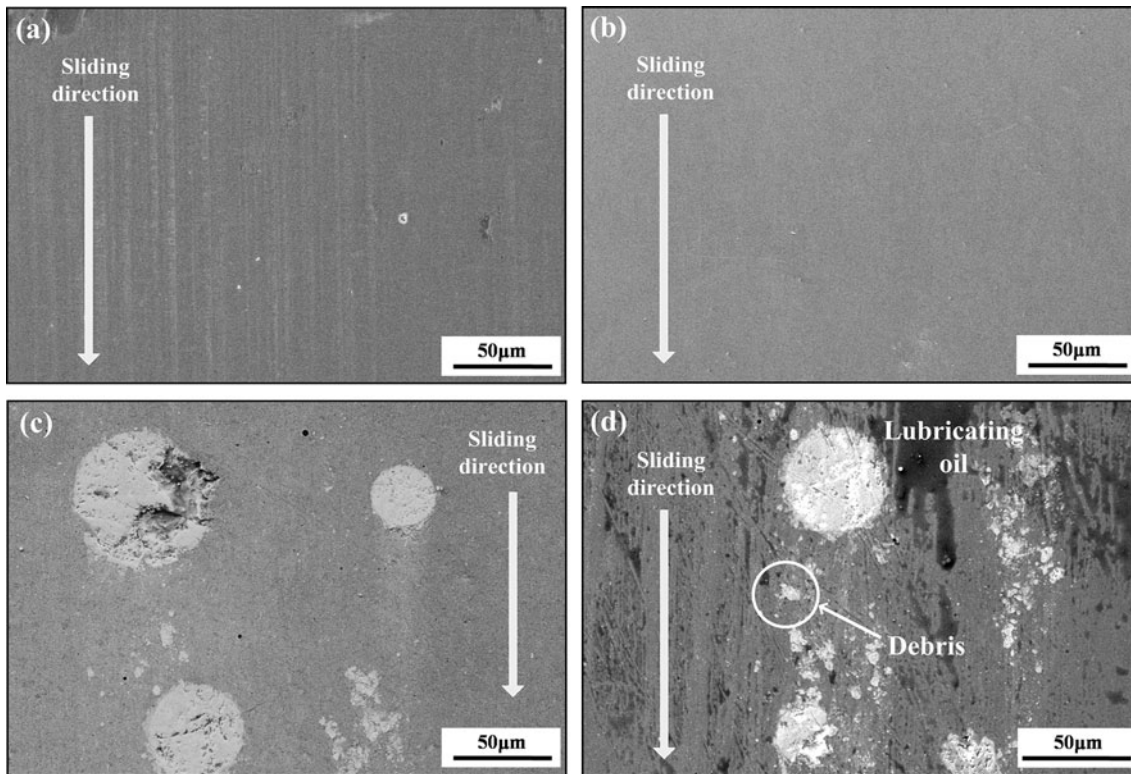
Fig. 8 Worn surface morphologies of (a) substrate material, (b) Ni alloy coating, (c) coating with 20 wt.% WC particles, and (d) coating with 60 wt.% WC particles after sliding tests
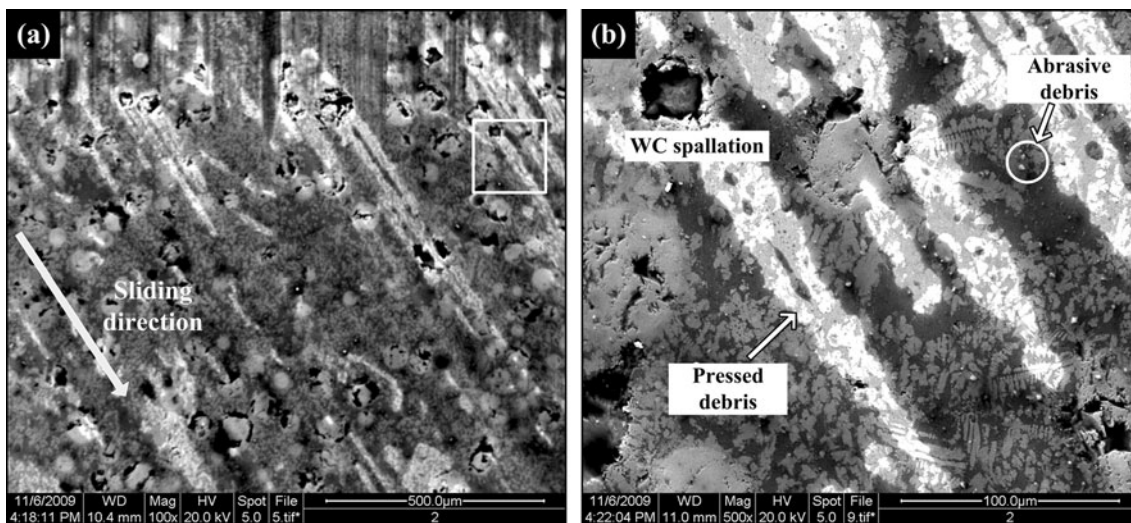

Fig. 9 SEM morphologies of the worn surface of coating with 80 wt.% WC particles, (a) overall view of the wear track; (b) higher magnification of rectangular area in (a) showing the debris and the spallation of WC particles

indicating the spallation of WC particle during sliding test. Obvious white bands appear near the WC particles along the sliding direction in Fig. 9(b), implying that a large amount of debris have been produced and pressed into the matrix. Figure 9(b) also shows the cavities resulting from the spallation of WC particle in higher magnification which can be attributed to the following reasons. First, the metallurgical bonding strength between WC particle and Ni matrix is comparatively low for the composite coatings with high WC content due to a lack of support of the carbide grains by the matrix phase. Second, when the volume fraction of WC in the coating is high,

the interaction between the adjacent hard particles will lead to high stress concentration near the edge of hard particles, which, in turn, promotes the spallation of WC particles.

4. Discussion

Previous work by Van Acker et al. (Ref 15) showed that the content of ceramic particles had an important influence on the sliding wear resistance of the particle reinforced composite coatings. From Fig. 7, it can be seen that the wear resistance of

WC/Ni composite coatings is higher than that of both Ni coating and 45# steel and the dependence of the wear resistance on the WC content is not necessarily monotonic. However, the magnitude of microhardness of WC/Ni coating generally increases with increasing the WC content in coating, as seen in Fig. 6. Hence, the sliding wear resistance and failure modes of the WC/Ni composite coatings are not only associated with their hardness, but also associated with their microstructure and toughness.

Generally, classification of failure modes can be made on the basis of surface observations of the worn coating surfaces. Previous studies showed that the classification of the wear mechanisms in sliding wear could be categorized into four modes, namely adhesive wear, abrasive wear, fatigue wear, and corrosive wear (Ref 20). However, only two failure modes are indentified in this study, namely, abrasive wear and fatigue wear. The coating specimens fail in either one of these types of mechanisms or a combination of two depending upon the microstructure of coatings with different contents of WC.

For the coatings with WC content lower than 40 wt.% in the feed powder, abrasive wear dominates the wear process of coatings, as revealed from the worn surface observation in Fig. 8(c) and (d). The WC particle reinforcement performs well to restrain abrasive wear. Therefore, the addition of WC particle effectively improves the wear resistance. For the coatings with high WC content, fatigue wear can been seen at the worn surface apart from abrasive wear. Due to the high volume of the hard particles, high stress concentration and poor interface bonding strength between the ceramic reinforcement and the surrounded matrix may be generated during the laser cladding process, accelerating the formation of fracture and spallation of WC particles under cyclic loading. Then, the hard WC debris as the three bodies entrap into the contact surfaces and aggravate the abrasive wear. In such a case, the wear resistance decreases with increasing the volume fraction of reinforcement phase when the WC content exceeds 40 wt.% in the feed powder. The coating with 40 wt.% WC particle reinforcement in the feed powder exhibits the best wear resistance under the lubrication sliding wear test conditions. Similar result has been obtained for tungsten reinforced composites by Wang et al. (Ref 21).

5. Conclusions

The present research focuses on the effect of content of reinforced WC particle on the microstructure and sliding wear resistance of laser cladded WC/Ni composite coatings on 45# steel substrates. It is found that the microstructure of the coatings with different contents of WC particle is homogeneous and free of pores and cracks. The interfacial bonding strength between the reinforced WC particle and the Ni matrix can be enhanced through the dissolution of WC at the edge of particles. The microhardness of WC/Ni coatings is obviously higher than that of substrate. With increasing the WC content, the microhardness of coatings generally increases. Sliding wear resistance of composite coatings is strongly dependent on the WC content within the coatings. When the WC content is lower than 40 wt.% in the feed powder, the wear resistance of coating increases with increasing WC content. The two-body abrasive wear is identified as the main wear mechanism. When the content of WC further increases, the wear resistance of coatings decreases. In

such a case, the fatigue wear and three-body abrasive wear can be identified as the main wear mechanisms.

References

1. S. Stewart, R. Ahmed, and T. Itsukaichi, Rolling Contact Fatigue of Post-Treated WC-NiCrBSi Thermal Spray Coatings, *Surf. Coat. Technol.*, 2005, **190**(2–3), p 171–189
2. S.H. Leigh and C.C. Berndt, Modelling of Elastic Constants of Plasma Spray Deposits with Ellipsoid-Shaped Voids, *Acta Mater.*, 1999, **47**(5), p 1575–1586
3. Z. Wang, A. Kulkarni, S. Deshpande, T. Nakamura, and H. Herman, Effects of Pores and Interfaces on Effective Properties of Plasma Sprayed Zirconia Coatings, *Acta Mater.*, 2003, **51**(18), p 5319–5334
4. B.J. Gill and R. Ctucker, Plasma Spray Coating Processes, *Mater. Sci. Technol.*, 1986, **2**(3), p 207–213
5. S. Deshpande, A. Kulkarni, S. Sampath, and H. Herman, Application of Image Analysis for Characterization of Porosity in Thermal Spray Coatings and Correlation with Small Angle Neutron Scattering, *Surf. Coat. Technol.*, 2004, **187**(1), p 6–16
6. Y.P. Kathuria, Some Aspects of Laser Surface Cladding in the Turbine Industry, *Surf. Coat. Technol.*, 2000, **132**(2–3), p 262–269
7. A.R. Nicoll, Self-fluxing Coatings for Stationary Gas Turbines, *Thin Solid Films*, 1982, **95**(3), p 285–295
8. T.S. Sidhu, S. Prakash, and R.D. Agrawal, Hot Corrosion Behaviour of HVOF- and Fe-Based Superalloys in Na_2SO_4–60% V_2O_5 Environment at 900 °C, *Acta Mater.*, 2006, **54**(3), p 773–784
9. Y. Liu, J. Koch, J. Mazumder, and K. Shibata, Processing, Microstructure, and Properties of Laser-Clad Ni Alloy FP-5 on Al Alloy AA333, *Metall. Mater. Trans. B*, 1994, **25**(3), p 425–434
10. P. Chivavibul, M. Watanabe, S. Kuroda, and K. Shinoda, Effects of Carbide Size and WC-Co Coatings, *Surf. Coat. Technol.*, 2007, **202**(3), p 509–521
11. B.S. Xu, Z.X. Zhu, S.N. Ma, W. Zhang, and W.M. Liu, Sliding Wear Behavior of Fe-Al and Fe-Al/WC Coatings Prepared by High Velocity Arc Spraying, *Wear*, 2004, **257**(11), p 1089–1095
12. M. Mohanty, R.W. Smith, M. De Bonte, J.P. Celis, and E. Lugscheider, Sliding Wear Behavior of Thermally Sprayed 75/25 Cr_3C_2/NiCr Wear Resistant Coatings, *Wear*, 1996, **198**(1–2), p 251–266
13. S.W. Huang, M. Samandia, and M. Brandt, Abrasive Wear Performance and Microstructure of Laser Clad WC/Ni Layers, *Wear*, 2004, **256**(11–12), p 1095–1105
14. H.H. Chen, C.Y. Xu, J. Chen, H.Y. Zhao, L. Zhang, and Z.T. Wang, Microstructure and Phase Transformation of WC/Ni60B Laser Cladding Coatings During Dry Sliding Wear, *Wear*, 2008, **264**(7–8), p 487–493
15. K. Van Acker, D. Vanhoyweghen, R. Persoons, and J. Vangrunderbeek, Influence of Tungsten Carbide Particle Size and Distribution on the Wear Resistance of Laser Clad WC/Ni Coatings, *Wear*, 2005, **258**(1–4), p 194–202
16. P. Wu, H.M. Du, X.L. Chen, Z.Q. Li, H.L. Bai, and E.Y. Jiang, Influence of WC Particle Behavior on the Wear Resistance Properties of Ni-WC Composite Coating, *Wear*, 2004, **257**(1–2), p 142–147
17. L. Dubourg, D. Ursescu, F. Hlawka, and A. Cornet, Laser Cladding of MMC Coatings on Aluminium Substrate: Influence of Composition and Microstructure on Mechanical Properties, *Wear*, 2005, **258**(11–12), p 1745–1754
18. Q.Q. Yang, T. Senda, and A. Ohmori, Effect of Carbide Grain Size on Microstructure and Sliding Wear Behavior of HVOF-Sprayed WC-12% Co Coatings, *Wear*, 2003, **254**(1–2), p 23–34
19. M.J. Tobar, C. Álvarez, J.M. Amado, G. Rodríguez, and A. Yáñez, Morphology and Characterization of Laser Clad Composite NiCrBSi-

WC Coatings on Stainless Steel, *Surf. Coat. Technol.*, 2006, **200**(22–23), p 6313–6317

20. J.T. Burwell, Survey of Possible Wear Mechanisms, *Wear*, 1957, **1**(2), p 119–141

21. H.M. Wang, D.Y. Luan, and L.X. Cai, Microstructure and Sliding-Wear Behavior of Tungsten-Reinforced W-Ni-Si Metal-Silicide In-Situ Composites, *Metall. Mater. Trans. A*, 2003, **34**(9), p 2005–2015